

Interpretation of the Processes ${}^3\text{He}(e, e'p){}^2\text{H}$ and ${}^3\text{He}(e, e'p)(pn)$ at High Missing Momenta

C. Ciofi degli Atti and L. P. Kaptari*

Department of Physics, University of Perugia and Istituto Nazionale di Fisica Nucleare, Sezione di Perugia, Via A. Pascoli, I-06123, Italy

(Received 26 March 2005; published 27 July 2005)

Using realistic three-body wave functions corresponding to the AV18 interaction, it is shown that the effects of the final state interaction in the exclusive processes ${}^3\text{He}(e, e'p){}^2\text{H}$ and ${}^3\text{He}(e, e'p)(pn)$, can be successfully treated in terms of a generalized eikonal approximation based upon the direct calculation of the Feynman diagrams describing the rescattering of the struck nucleon. The relevant role played by the double rescattering contribution at high values of the missing momentum is illustrated.

DOI: 10.1103/PhysRevLett.95.052502

PACS numbers: 24.10.-i, 25.10.+s, 25.30.Dh, 25.30.Fj

Recent experimental data from Jlab on exclusive electro-disintegration of ${}^3\text{He}$ [1–3] are at present the object of intense theoretical activity (see [4–6] and References therein). In Ref. [5] (to be quoted hereafter as *I*) the 2-body break up (*2bbu*) and 3-body break up (*3bbu*) channels, ${}^3\text{He}(e, e'p){}^2\text{H}$ and ${}^3\text{He}(e, e'p)(pn)$ respectively, have been calculated within the following approach: (i) initial state correlations have been taken care of by the use of the state-of-the-art few-body wave functions [7] corresponding to the AV18 interaction [8]; (ii) final state interactions (FSIs) have been treated by a generalized Eikonal approximation (GEA) [9]. GEA represents an extended Glauber-type approach (GA) [10] based upon the evaluation of the relevant Feynman diagrams that describe the rescattering of the struck nucleon in the final state, in analogy with the Feynman diagrammatic approach developed for the treatment of elastic hadron-nucleus scattering [11,12]. The Feynman diagrams pertaining to the process ${}^3\text{He}(e, e'p)X$ (with $X = {}^2\text{H}$ or (pn)) are shown in Fig. 1. In *I* the theoretical calculations have been compared with the preliminary Jlab data [3] covering a region of missing momentum and energy with $p_m \leq 0.6$ GeV/*c* and $E_m \leq 100$ MeV. Since the recently published data [1,2] extend to higher values of the missing momentum ($p_m \leq 1.0$ GeV/*c*), which have not been considered in *I*, the aim of this paper is to analyze our predictions in the entire range of missing momentum $p_m \leq 1.2$ GeV/*c*. We will first of all argue that the missing momentum dependence of the *2bbu* channel cross section, namely, its changes of slope, can be a signature of different orders of final state rescattering and, secondly, we will show that our fully parameter free calculation can reproduce the experimental data in the entire range of missing momentum, with the high missing momentum behavior ($p_m \geq 0.6$ GeV/*c*) mainly governed by double scattering effects. Although the details of the theoretical approach can be found in *I*, it is worth briefly recalling the basic assumptions underlying GA and GEA. The former is based upon the following approximations: (i) the nucleon-nucleon (NN) scattering amplitude is obtained within the eikonal approximation; (ii) the nucleons of the spectator system $A - 1$ are sta-

tionary during the multiple scattering with the struck nucleon (*frozen approximation*); (iii) only perpendicular momentum transfer components in the NN scattering amplitude are considered. In GEA the *frozen approximation* is partly removed by taking into account the excitation energy of the $A - 1$ system, resulting in a longitudinal momentum transfer dependence of the standard GA profile function. Let us omit (see *I* for details) any discussion concerning the assumptions and approximations which, starting from the Feynman diagrams shown in Fig. 1, allow one to obtain a calculable cross section, and let us instead write down the final expression for the latter; for the processes ${}^3\text{He}(e, e'p)X$, one has

$$\frac{d^6\sigma}{dE'd\Omega'd\mathbf{p}_m} = K(Q^2, x, \mathbf{p}_m) \sigma^{eN}(\bar{Q}^2, \mathbf{p}_m) P_{\text{He}}^{\text{FSI}}(\mathbf{p}_m, E_m), \quad (1)$$

where $Q^2 = -q^2 = -(k - k')^2 = \mathbf{q}^2 - q_0^2 = 4EE'\sin^2\theta/2$ is the four-momentum transfer; $x = Q^2/2M_N q_0$ is the Bjorken scaling variable; $\bar{Q}^2 = \mathbf{q}^2 - \bar{q}_0^2$ ($\bar{q}_0 = q_0 + M_3 - \sqrt{(\mathbf{k}_1^2 + (M_2^f)^2) - \sqrt{\mathbf{k}_1^2 + M_N^2}}$); M_3 is the mass of ${}^3\text{He}$ and $M_2^f = M_2 + E_2^f$ the mass of the two-nucleon system in the final state with intrinsic excitation energy E_2^f ; $\mathbf{p}_m = \mathbf{q} - \mathbf{p}_1 = \mathbf{P}_2$ and $E_m = E_{\text{min}} + E_2^f$ are

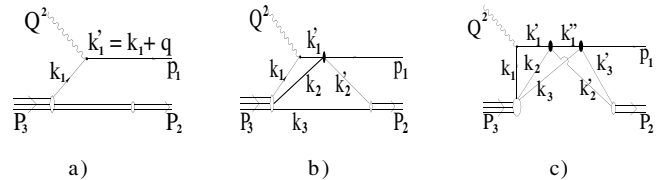


FIG. 1. The Feynman diagrams representing the PWIA (a), the single (b), and double (c) rescattering in the processes ${}^3\text{He}(e, e'p){}^2\text{H}$ and ${}^3\text{He}(e, e'p)(pn)$. In the former case the final two-nucleon state is a deuteron with momentum \mathbf{P}_2 , whereas in the latter case the final state represents two nucleons in the continuum with momenta \mathbf{p}_2 and \mathbf{p}_3 , with $\mathbf{P}_2 = \mathbf{p}_2 + \mathbf{p}_3$. The trivial single and double rescattering diagrams with nucleons “2” and “3” interchanged are not drawn. The black oval spots denote the elastic NN scattering matrix.

the missing momentum and energy, respectively; the threshold and intrinsic excitation energies are $E_{\min} = E_3 - E_2$ ($E_{\min} = E_3$) and $E_2^f = 0$ ($E_2^f = \mathbf{t}^2/M_N$, $\mathbf{t} = \frac{\mathbf{k}_2 - \mathbf{k}_3}{2}$) for the $2bbu$ ($3bbu$) channel, respectively; $E_2(E_3)$ are the (positive) ground-state energy of ${}^2\text{H}$ (${}^3\text{He}$). The quantity $K(Q^2, x, \mathbf{p}_m)$ is a kinematical factor, $\sigma^{eN}(\bar{Q}^2, \mathbf{p}_m)$ is the cross section describing electron scattering by an off-shell nucleon, and, eventually, $P_{\text{He}}^{\text{FSI}}(\mathbf{p}_m, E_m)$ is the distorted spectral function containing the effects from initial state correlations and FSI; within GEA, one has

$$P_{\text{He}}^{\text{FSI}}(\mathbf{p}_m, E_m) = \frac{1}{(2\pi)^3} \frac{1}{2} \sum_f \sum_{\mathcal{M}_3, \mathcal{M}_2, s_1} \left| \sum_{n=0}^2 \mathcal{T}_3^{(n)}(\mathcal{M}_3, \mathcal{M}_2, s_1; f) \right|^2 \delta(E_m - (E_2^f + E_{\min})), \quad (2)$$

where \mathcal{M}_3 , \mathcal{M}_2 , and s_1 are the magnetic quantum numbers of ${}^3\text{He}$, of the two-nucleon system in the final state, and of the struck nucleon in the continuum, respectively; the quantity $\mathcal{T}_3^{(n)}(\mathcal{M}_3, \mathcal{M}_2, s_1; f)$, which can be called the *reduced (Lorentz index independent) amplitudes* (see, e.g., [1]), results from the evaluation of the Feynman diagrams of Fig. 1, with $\mathcal{T}_3^{(0)}$ corresponding to the plane wave impulse approximation (PWIA) (Fig. 1(a)), $\mathcal{T}_3^{(1)}$ to the single-rescattering FSI (Fig. 1(b)), and $\mathcal{T}_3^{(2)}$ to the double rescattering FSI (Fig. 1(c)); the explicit evaluation of the diagrams yields

$$P_{\text{He}}^{\text{FSI}}(\mathbf{p}_m, E_m) = P_{\text{gr}}^{\text{FSI}}(\mathbf{p}_m, E_m) + P_{\text{ex}}^{\text{FSI}}(\mathbf{p}_m, E_m), \quad (3)$$

where the first and the second terms describing the $2bbu$ and the $3bbu$ channel, respectively, are

$$P_{\text{gr}}^{\text{FSI}}(\mathbf{p}_m, E_m) = \frac{1}{(2\pi)^3} \frac{1}{2} \sum_{\mathcal{M}_3, \mathcal{M}_2, s_1} \left| \int e^{i\mathbf{p}\mathbf{p}_m} \chi_{1/2s_1}^\dagger \Psi_D^{\mathcal{M}_2 \dagger}(\mathbf{r}) S_{\Delta}^{\text{FSI}}(\mathbf{p}, \mathbf{r}) \Psi_{\text{He}}^{\mathcal{M}_3}(\mathbf{p}, \mathbf{r}) d\mathbf{p} d\mathbf{r} \right|^2 \delta[E_m - (E_3 - E_2)], \quad (4)$$

$$P_{\text{ex}}^{\text{FSI}}(\mathbf{p}_m, E_m) = \frac{1}{(2\pi)^3} \frac{1}{2} \sum_{\mathcal{M}_3, s_{23}, s_1} \int \frac{d^3\mathbf{t}}{(2\pi)^3} \left| \int e^{i\mathbf{p}\mathbf{p}_m} \chi_{1/2s_1}^\dagger \Psi_{np}^{\dagger}(\mathbf{r}) S_{\Delta}^{\text{FSI}}(\mathbf{p}, \mathbf{r}) \Psi_{\text{He}}^{\mathcal{M}_3}(\mathbf{p}, \mathbf{r}) d\mathbf{p} d\mathbf{r} \right|^2 \delta\left(E_m - \frac{\mathbf{t}^2}{M_N} - E_3\right) \quad (5)$$

with $\Psi_{\text{He}}^{\mathcal{M}_3}(\mathbf{p}, \mathbf{r})$, $\Psi_D^{\mathcal{M}_2}(\mathbf{r})$, and $\Psi_{np}^{\dagger}(\mathbf{r})$, being the wave functions of ${}^3\text{He}$, of the deuteron, and of the np pair in the continuum, respectively. Here, the FSI factor S_{Δ}^{FSI} , which describes the single and double rescattering of nucleon “1,” has the form $S_{\Delta}^{\text{FSI}}(\mathbf{p}, \mathbf{r}) = S_{(1)}^{\text{FSI}}(\mathbf{p}, \mathbf{r}) + S_{(2)}^{\text{FSI}}(\mathbf{p}, \mathbf{r})$ with the single and double rescattering contributions given, respectively, by

$$S_{(1)}^{\text{FSI}}(\mathbf{p}, \mathbf{r}) = 1 - \sum_{i=2}^3 \theta(z_i - z_1) e^{i\Delta_i(z_i - z_1)} \Gamma(\mathbf{b}_1 - \mathbf{b}_i); \quad (6)$$

$$S_{(2)}^{\text{FSI}}(\mathbf{p}, \mathbf{r}) = \Gamma(\mathbf{b}_1 - \mathbf{b}_2) \Gamma(\mathbf{b}_1 - \mathbf{b}_3) [\theta(z_2 - z_1) \theta(z_3 - z_2) e^{-i\Delta_3(z_2 - z_1)} e^{-i(\Delta_3 - \Delta_2)(z_3 - z_1)} + \theta(z_3 - z_1) \theta(z_2 - z_3) e^{-i\Delta_2(z_3 - z_1)} e^{-i(\Delta_2 - \Delta_3)(z_2 - z_1)}], \quad (7)$$

where $\Delta_i = (q_0/|\mathbf{q}|)(E_{\mathbf{p}_i} - E_{\mathbf{k}_i'})$ and $\Delta_z = (q_0/|\mathbf{q}|)E_m$ [9]. The usual Glauber FSI factor [13]

$$S_G^{\text{FSI}}(\mathbf{p}, \mathbf{r}) = \prod_{i=2}^3 [1 - \theta(z_i - z_1) \Gamma(\mathbf{b}_i - \mathbf{b}_1)] \quad (8)$$

is recovered by setting $\Delta_i = \Delta_z = 0$, whereas by also setting $\Gamma = 0$, the usual spectral function is obtained. An inspection of Eqs. (6) and (7) shows that by taking into consideration the factor Δ_z , the *frozen approximation* is partly removed, resulting in a longitudinal momentum

transfer correction term to the standard profile function of GA. Note that the conditions for the validity of the factorized form (1) for the cross section, have been discussed in detail in Ref. [5] (Appendix B), showing that if the spin-flip part of the NN scattering amplitude is small and the momentum transfer in the final state rescattering $|\mathbf{k}| \ll |\mathbf{p}_1|$, as it is the case for the sharply forward peaked NN scattering amplitude used in Glauber-type calculations, then factorization should occur to a large extent. Concerning the numerical results we have obtained, it is also worth mentioning that we found the effects due to the Δ 's appearing in Eqs. (6) and (7) to be of the order of few percent, since, as explained in Ref. [5], the experimental data we are considering are practically at perpendicular kinematics whereas the Δ 's mainly affect the longitudinal momentum distributions (see also Ref. [9]).

We have used Eqs. (1) and (3) to calculate the cross sections of the processes ${}^3\text{He}(e, e'p){}^2\text{H}$ and ${}^3\text{He}(e, e'p) \times (np)$. All calculations have been performed in the reference frame where the axis z is directed along the momentum of the struck nucleon \mathbf{p}_1 . The common well-known parameterization of the profile function $\Gamma(\mathbf{b}) = \sigma_{\text{NN}}^{\text{tot}}(1 - i\alpha_{\text{NN}}) \times \exp(-\mathbf{b}^2/2b_0^2)/(4\pi b_0^2)$ has been used, where $\sigma_{\text{NN}}^{\text{tot}}$ is the total NN cross section, α_{NN} the ratio of the real to imaginary part of the forward NN amplitude, and b_0 the slope of the differential elastic NN cross section; the energy dependent values of these quantities have been taken from Ref. [14]. The electron-nucleon cross section

$\sigma_{cc1}^{eN}(\vec{Q}^2, \mathbf{p}_m)$ is the one of Ref. [15]. All two- and three-body wave functions are direct solutions of the non relativistic Schrödinger equation; therefore our calculations are fully parameter free. It should be stressed, in this connection, that besides the GEA no further approximations have been made in the evaluation of the single and double rescattering contributions to the FSI: proper intrinsic coordinates have been used and the energy dependence of the profile function has been taken into account in the properly chosen c.m. system of the interacting pair.

The results of our calculation for the $2bbu$ channel, which are compared with the experimental data in Fig. 2, deserve the following comments: (i) the missing momentum dependence of the experimental cross section clearly exhibits different slopes that are reminiscent of the slopes observed in elastic hadron-nucleus scattering at intermediate energies (see, e.g., Ref. [16]); (ii) our calculations, as clearly illustrated in Fig. 2, demonstrate that these slopes are indeed related to multiple scattering in the final state; (iii) without any free parameter, a very satisfactory agreement between experimental data and theoretical calculations can be obtained, which means that in the energy-momentum range covered by the data, FSI can be de-

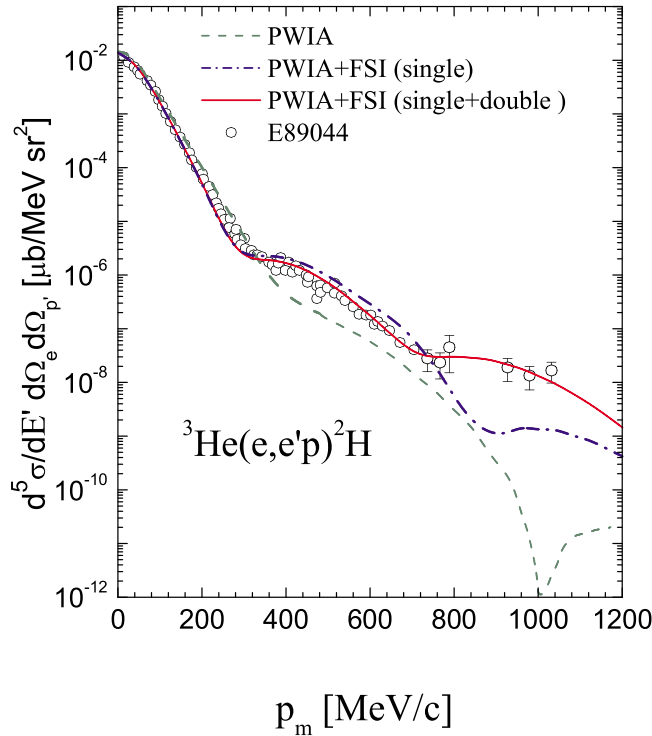


FIG. 2 (color online). The experimental data from JLab [1] ($Q^2 = 1.55$ (GeV/c) 2 , $x = 1$) on the $2bbu$ process ${}^3\text{He}(e, e'p)^2\text{H}$ vs the missing momentum p_m , compared with our theoretical results. The dashed line corresponds to the PWIA [Eq. (4) with $S_{\Delta}^{\text{FSI}} = 1$], the dot-dashed line includes the FSI with single rescattering ($S_{\Delta}^{\text{FSI}} = S_{(1)}^{\text{FSI}}$), and the solid line includes both single and double rescattering ($S_{\Delta}^{\text{FSI}} = S_{(1)}^{\text{FSI}} + S_{(2)}^{\text{FSI}}$) (three-body wave function from [7], AV18 interaction [8]).

scribed within the GEA. In order to better understand the role played by multiple rescattering in the final state, we show in Fig. 3 the separate contributions of the PWIA, the single and double rescattering contributions, and the interference contributions. It can be seen that at $p_m \leq 0.2$ GeV/c, the cross section is mainly governed by the PWIA, at $0.2 \leq p_m \leq 0.6$ GeV/c, by the single-rescattering FSI, and at $p_m \geq 0.6$ GeV/c, by the double rescattering FSI, with the interference terms also providing relevant contributions in specific regions. The results of the $3bbu$ channel calculations are shown in Fig. 4, and they also appear to be in good agreement with the experimental data [2], although a systematic underestimation of the latter is observed at $p_m = 820$ MeV/c and $E_{\text{rel}} \leq 110$ MeV. The origin of such a disagreement, which might be due to meson exchange current effects [17], nonfactorizing contributions to the cross section [6], charge-interchange amplitudes, and other effects which are not included in our approach, is under investigation.

To sum up, in this Letter we have extended the approach of I to the calculation of the high missing momentum part of the processes ${}^3\text{He}(e, e'p)^2\text{H}$ and ${}^3\text{He}(e, e'p)(pn)$. We have found that our theoretical predictions provide a very satisfactory agreement with the Jlab data. Such an agreement cannot be considered fortuitous, for it has been found to occur in the process ${}^2\text{H}(e, e'p)n$, as well as in the processes ${}^3\text{He}(e, e'p)^2\text{H}$ and ${}^3\text{He}(e, e'p)(pn)$ in kinematical conditions differing from the Jlab ones [18] (see I). A recent calculation [17] of the same processes we have considered in this Letter also produced an overall good agreement with the experimental data. The calculation of [17] is based upon the diagrammatic expansion developed in [19], and the agreement with the experimental data at high values of the missing momentum is achieved by a

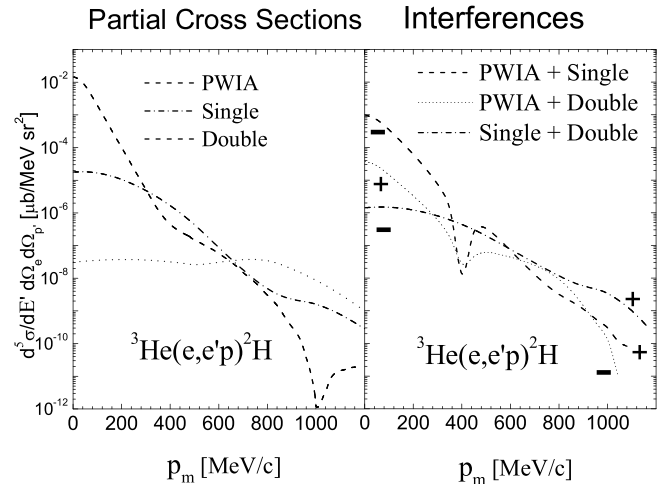


FIG. 3. The partial cross sections (left) and the interference contributions (right) in the process ${}^3\text{He}(e, e'p)^2\text{H}$ calculated including the full FSI. The continuous curve in Fig. 2 is obtained by summing the partial cross sections and the interference contributions with the proper sign.

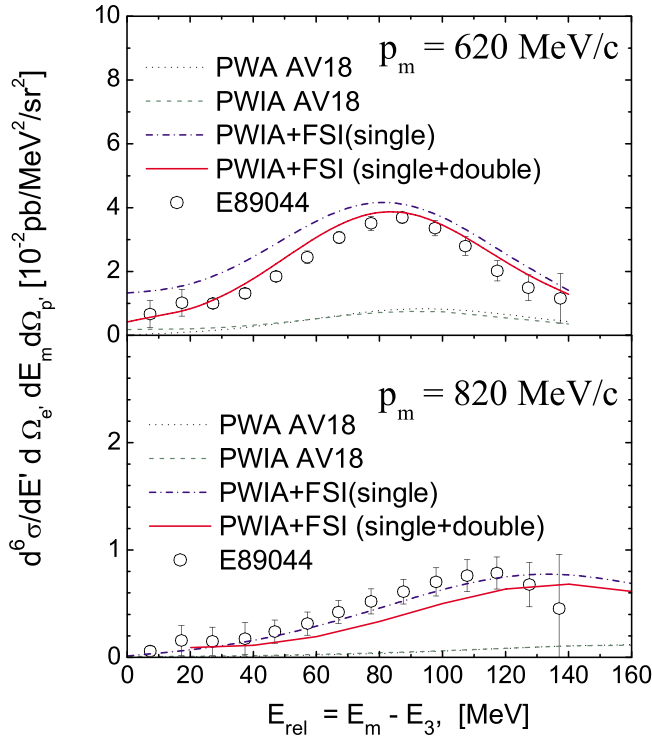


FIG. 4 (color online). The differential cross section of the $3bbu$ process ${}^3\text{He}(e, e'p)(np)$ [2], plotted, for fixed values of p_m , vs the excitation energy of the two-nucleon system in the continuum $E_{\text{rel}} = \mathbf{t}^2/M_N = E_2^f = E_m - E_3$. The theoretical calculations correspond to Eq. (5) and the meaning of the various curves is the same as in Fig. 2. The curves labeled PWA do not include any FSI.

three-body mechanism in which the virtual photon is absorbed by a nucleon at rest which propagates emitting a meson, which is reabsorbed by the spectator nucleon pair. A careful comparison of our results and the ones of Ref. [17] reveals, however, several differences whose origin has to be clarified in order to better understand the basic reaction mechanism of the process. To this end, it would be extremely useful to access: (i) experimental data at higher values of p_m for the process ${}^3\text{He}(e, e'p)X$ and (ii) experimental data for the process ${}^4\text{He}(e, e'p){}^3\text{H}$, whose

p_m dependence, within the GEA, looks different from the one of the process ${}^3\text{He}(e, e'p){}^2\text{H}$ [20].

The authors are indebted to A. Kievsky for making available the variational three-body wave functions of the Pisa Group. Useful discussions with M. Sargsian, R. Schiavilla, and M. Strikman are gratefully acknowledged. L. P. K. is indebted to the University of Perugia and INFN, Sezione di Perugia, for a grant and for warm hospitality.

*On leave from Bogoliubov Laboratory of Theoretical Physics, 141980, JINR, Dubna, Russia

- [1] M. M. Rvachev *et al.*, Phys. Rev. Lett. **94**, 192302 (2005).
- [2] F. Benmokhtar *et al.*, Phys. Rev. Lett. **94**, 082305 (2005).
- [3] A. Saha, M. Epstein, and E. Voutier, TJLAB Experiment E-89-044 (unpublished).
- [4] J.-M. Laget, nucl-th/0410003.
- [5] C. Ciofi degli Atti and L. P. Kaptari, Phys. Rev. C **71**, 024005 (2005).
- [6] R. Schiavilla (private communication).
- [7] A. Kievsky, S. Rosati, and M. Viviani, Nucl. Phys. **A551**, 241 (1993).
- [8] R. B. Wiringa, V. G. J. Stoks, and R. Schiavilla, Phys. Rev. C **51**, 38 (1995).
- [9] L. L. Frankfurt, M. M. Sargsian, and M. I. Strikman, Phys. Rev. C **56**, 1124 (1997). M. M. Sargsian, T. V. Abrahamyan, M. I. Strikman, and L. L. Frankfurt, Phys. Rev. C **71**, 044614 (2005).
- [10] R. J. Glauber, in *Lectures in Theoretical Physics*, edited by W. E. Brittin *et al.* (Interscience Publishers, Inc., New York, 1959).
- [11] V. N. Gribov, Sov. Phys. JETP **30**, 709 (1970).
- [12] L. Bertocchi, Nuovo Cimento Soc. Ital. Fis. A **11**, 45 (1972).
- [13] N. N. Nikolaev, J. Speth, and B. G. Zakharov, J. Exp. Theor. Phys. **82**, 1046 (1996).
- [14] R. A. Arndt *et al.*, (SAID) Partial-Wave Analysis Facility, <http://said.phys.vt.edu/>.
- [15] T. de Forest, Jr., Nucl. Phys. **A392**, 232 (1983).
- [16] G. Alberi and G. Goggi, Phys. Rep. **74**, 1 (1981).
- [17] J.-M. Laget, nucl-th/0410003 [Phys. Rev. C (to be published)].
- [18] C. Marchand *et al.*, Phys. Rev. Lett. **60**, 1703 (1988).
- [19] J.-M. Laget, Phys. Rev. C **38**, 2993 (1988).
- [20] C. Ciofi degli Atti, H. Morita, and L. Kaptari (to be published).